IEEE Access
Multidisciplinary ⋮ Rapid Review ⋮ Open Access Journal

Received 1 May 2024, accepted 16 May 2024, date of publication 22 May 2024, date of current version 30 May 2024.

Digital Object Identifier 10.1109/ACCESS.2024.3404046

RESEARCH ARTICLE

RadRCom: A Relay-Assisted Radar Communication System Design Framework

SOUMITA NASKAR, (Graduate Student Member, IEEE), AND AMIT KUMAR DUTTA, (Member, IEEE)

G. S. Sanyal School of Telecommunication, Indian Institute of Technology at Kharagpur, Kharagpur 721302, India

Corresponding author: Amit Kumar Dutta (amitkdutta@yahoo.co.in)

This work was supported by MeitY, Government of India under Grant 13(44)/2020-CC&BT.

ABSTRACT This study introduces the novel communication topology, namely RadRCom, integrating radar and relay-assisted communication systems for single antenna configuration as a proof of concept. While simultaneous radar and communication operations within the same spectrum gain momentum, our work advances this concept by incorporating relay assistance, particularly crucial in applications like vehicle-to-anything (V2X) communication. The inclusion of relays significantly enhances communication system performance, addressing challenges such as interference management between radar, relay, and communication nodes. This topology attracts three design challenges such as optimal radar waveform, relay parameters and communication system parameters. However, the key bottlenecks are the interference from radar to the relay and communication receiver and similarly the one from communication transmitter and relay node to the radar. Therefore, the work addresses these challenges simultaneously meeting the quality of service. Our proposed RadRCom system optimizes radar waveform and relay parameters to improve signal-to-interference noise ratio (SINR) at the radar and mean square error (MSE) of data transmission. We introduce two frameworks for parameter design, i.e, radar-centric and relay-centric ones. We take a sub-optimal iterative approach to address the computational complexity. Numerical simulations are performed to evaluate the performances of the proposed RadRCom system with the proposed algorithms.

INDEX TERMS Radar, transceiver, RadRCom, coexistence, relay, optimization, BER, MSE, SINR, KPI, RLLC, detection, PFA.

I. INTRODUCTION

The remarkable growth in tele-traffic over the past decade has propelled the advancement of next-generation cellular systems, particularly the fifth generation (5G) and beyond [1], [2], [3]. This surge in demand necessitates a larger spectrum allocation for communication systems, with spectrum sharing among multiple transceiver systems becoming commonplace. With the emergence of 5G and the Internet of Things (IoT), diverse applications such as automotive, imaging, and vehicular data transmission have garnered significant attention, given their requirement for both radar and communication functionalities [4]. Consequently, due to its scarcity, the sharing of spectrum between radar and communication systems has become imperative. This marks the onset of a new era in research, where the coexistence of radar and communication systems is being comprehensively examined, often referred to as radar-communication systems or RadCom. Furthermore, existing wireless standards are accommodating the coexistence of radar and communication systems [5]. On the other hand, relay technology has garnered significant attention for its ability to extend the coverage area of transmitted signals over considerable distances [6], [7]. Beyond increasing range, relays also play a crucial role in ensuring the reliability of communication links. This significance is particularly pronounced in automotive applications of radar-communication systems, where the potential for link failures due to channel unavailability is a pertinent concern. Recognizing the importance of addressing such challenges, we have introduced relay functionality within the RadCom system in this study. By integrating relays, our aim is to not only enhance the communication

The associate editor coordinating the review of this manuscript and approving it for publication was Pinjia Zhang.

© 2024 The Authors. This work is licensed under a Creative Commons Attribution-NonCommercial-NoDerivatives 4.0 License.
For more information, see https://creativecommons.org/licenses/by-nc-nd/4.0/

radius but also ensure the reliability of communication links, thus advancing the capabilities of RadCom systems.

Literature Survey: Extensive literature exists in the field of RadCom, where the coexistence of two fields is becoming a reality [5], [8]. Work in [9] proposes an excellent trade-off between the radar and a communication network's co-existence with stochastic geometry. Pioneering work in [10] proposes a RadCom system with new waveform based on orthogonal frequency division multiplexing (OFDM). It optimizes the system based on information theoretic aspect. A multi-antenna-based beamforming is proposed in [11] in a cellular network with radar coexistence. In a similar line, work in [12] proposes a communication system aware waveform design in multi-antenna RadCom system with good beam pattern design as well. Interfering channel estimation is proposed in [13] with maximum likelihood (ML) method. A dual function radar and communication system has been proposed in [14], where the same waveform will be used for radar in main lobe and information bearing communication system in side-lobe. A comprehensive RadCom work is proposed for future sixth generation (6G) in [3]. The work in [15] proposes a massage passing algorithm for efficient detection in communication system sharing radar spectrum. Authors in [16] and [17] propose joint design of MIMO transceiver and radar system, while work in [18] proposes a MIMO based full-duplex transceiver design with radar spectrum sharing. Authors in [19] proposes the co-existence of matrix completion MIMO RadCom with spectrum sharing. In surveillance application, RadCom finds excellent work in [20], where time synchronization is not assumed. Works in [21], [22], and [23] propose a RadCom system, where various waveform design aspects under various constraints are considered with multiple targets. A mmWave-based joint radar and communication system has also been proposed in [24] based on the OFDM waveform. Reference [25] addresses an OFDM based RadCom system where synchronization issues in time and frequency are analyzed. Work in [26] proposes a multi-user MIMO communication system design along with the radar system. A recent work in RadCom [27] considers a waveform design based on the detection probability. Additionally, unlike the coexistence scenario, in [28], authors have introduced a Pareto optimization framework designed for a multi-antenna dual-functional radar-communication (DFRC) system that focuses on joint radar communication scenarios. This system involves a single transmitter equipped with multiple antennas, enabling communication with multiple users and simultaneous detection of radar targets.

Furthermore, an extensive body of literature is dedicated to communication utilizing relay technology. Most of the relay design aspects include the optimal design of the precoder at the transmitter or source node (SN), relay gain at the relay node (RN) and equalizer at the receiver or destination node (DN) based on various design criteria. The work in [29] proposes a relay based on the mean square error (MSE) criterion for a single antenna system, while works in [30], [31] propose relay design for multiple-input multiple-output (MIMO) system. Authors in [6] propose relay design based on the bit error ratio (BER) criterion for the MIMO system. A recent work in [32] considers a secure mmWave relay transmission, which can be used in vehicular-to-anything (V2X) system.

Key gap in RadCom: However, the above works in RadCom do not consider relay at communication system. Though, relay has played an active role in radar waveform design [33] or in communication system individually, it is still not used in the context of joint radar and communication system design to the best of authors' knowledge. Therefore, to increase the reach of the radar communication system, a relay is proposed in this new topology.

Contributions: Given this background, the contributions of this work are as follows

1) We propose a new communication topology, where radar and relay assisted communication system would co-exist in the same spectrum in a cooperative manner such that quality of service (QoS) can be maintained at radar and communication system. This system model is the first proposal to the best of authors' knowledge. We propose to jointly design a waveform for the radar and the relay gain for the amplify-forward relay. We have assumed single antenna for radar and communication nodes as this is the first basic paper as proof of concept. We term this configuration as radar-relay-communication (RadRCom) system.
2) We consider signal-to-interference plus noise (SINR) and MSE as the QoS parameters at the radar and communication receiver, respectively in line with several RadCom works [27] to design radar waveform and other communication design parameters. A sub-optimal optimization framework is contemplated in both the cases. At first, a radar centric design is proposed, where SINR at the radar is maximized with along with other standard radar and relay parameters constraints. As the problem is non-convex and complexity computation is high, we propose a sub-optimal iterative solution with lesser complexity. This is extended to the relay centric scenario as well, where MSE of relay is minimized with various radar and relay parameters constraints.
3) We have done a performance analysis with respect to the detection probability at the radar considering all the interference statistics. We have also analyzed the symbol-error-rate (SER) at the communication receiver considering all the radar interference and fading.

Organization of the paper: The rest of this paper is organized as follows. Section II describes the system models for radar system and relay-assisted communication system. Section III designs the cost function and constraints for optimization statements. Section IV proposes the optimization framework and algorithm design to solve the optimization. Next, an analysis of the radar performance and SER

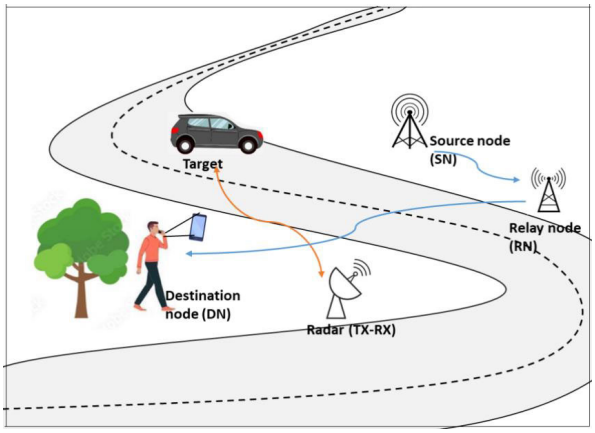

FIGURE 1. Coexistence of radar and relay assisted communication system having a target and SN, RN, DN with single antenna.

performance are derived in Section V. Finally, numerical results and conclusions are provided in Sections VI and VII, respectively.

Mathematical Notations: Some mathematical notations and symbols used in this article are described below.

$\mathbb{C}$, $\mathbb{C}^n$, $\mathbb{C}^{m\times n}$: Set of complex number, vector, and matrices.
$||\mathbf{A}||_{\mathbf{p}}$: p-norm of matrix A.
$\sigma(\mathbf{A})$: Eigenvalue spectrum of the operator $\mathbf{A}$.
$Tr(\mathbf{A})$: Trace of matrix $\mathbf{A}$.
$diag(\mathbf{v})$: Diagonal matrix with vector $\mathbf{v}$ in diagonal.
$dim(\mathbf{S})$: Dimension of the matrix $\mathbf{S}$.
x, $\mathbf{x}$, $\mathbf{X}$: Scalar, vector and matrix quantity.
$\mathbb{R}$, $\mathbb{C}$, $\mathbb{Z}$: Set of real, complex and integer numbers.
$\mathbf{A}^\dagger$, $\mathbf{a}^\dagger$: Complex conjugate transpose of the matrix "$\mathbf{A}$", and vector "$\mathbf{a}$", respectively.
$\mathbb{E}$: Expectation operator.
$[N]$: Set of natural numbers $1, 2, \ldots, N$.

II. SYSTEM MODEL

The system model of the proposed RadRCom is presented in FIGURE 1, which shows the co-existence of radar and relay assisted communication system. The system is assumed to consist of one target, a radar system, one communication source node or SN, a relay node or RN and a destination node or DN. The data flow diagram is shown in the diagram, which is downlink for the communication receiver. The SN will send data to DN only via RN. We assume that there is no direct link between SN and DN. In this work, we assume single antenna system for all the nodes along with the radar. The RN is part of the communication system to enhance the reach of the signal. We assume that the radar is a pulsed-coded radar, where T_p denotes the pulse repetition time and T_c is the duration of each code within a pulse. Let us assume that K is the total number of codes in a pulse. Hence, the pulse duration is $T_p \triangleq KT_c$. Let us assume that $\mathbf{c}_r = [c_1\ c_2\ \ldots c_K]^T$ denotes the code sent serially during the KT_c time. We assume a half-duplex relay as mentioned before. The sampling time of baseband data is assumed to be T_c at the communication

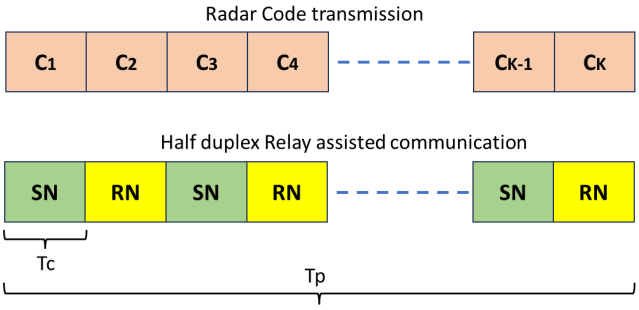

FIGURE 2. A complete frame timing is shown with pulse duration and relay transmission scheme.

system, so that it occupies a total bandwidth (BW) of $\frac{1}{T_c}$, which is the same for the radar. Let us assume that radar and communication systems are time-synchronized. We will consider data stream of K samples from both radar and communication system. The data transmission scheme of both radar and relay is shown in FIGURE 2, where SN and RN data transmissions are shown in alternate time slot due to half-duplex transmission nature. Whereas, the radar code occupies the whole K number of data slots.

On the other hand, let us assume that α is the square root of relay power gain at the RN and β is the equalizer parameter at the DN. We now consider the baseband sampled data model for radar and relay systems. Let us assume that SN transmits information data serially only at the odd position of K pulse duration as $\mathbf{x}_t = [x_1\ 0\ x_2\ 0 \ldots x_L]^T$. The RN transmits data at the even positions as $\mathbf{r}_r = [0\ r_1\ \ 0\ r_2 \ldots 0]^T$. This mechanism is done to support the half-duplex relay.

A. RADAR DATA MODEL

As radar sends pulses serially and receives them serially from a target, we denote the received signal as $\mathbf{y}_r \in \mathbb{C}^{K\times 1}$. Let us assume that h_c is the channel gain between target and the radar comprehending the path delay, h_1 is the channel between the radar and the SN, h_2 is the channel between radar and RN. All these channel coefficients are assumed to have single tap only. Ignoring the effect of clutter for the time being, the radar received signal $\mathbf{y_r}$ can be expressed as

$$\mathbf{y}_r = h_c\mathbf{c}_r + h_1\mathbf{x}_t + h_2\mathbf{r}_r + \mathbf{n}_r, \tag{1}$$

where $\mathbf{n}_r$ is the additive white Gaussian noise vector with each element having zero-mean independent and identical distribution with variance σ_r^2.

B. COMMUNICATION SYSTEM DATA MODEL

Considering K being an even case scenario, it will make $L = K/2$ and hence $\mathbf{x}_t^o$ is the collection of odd-positioned data of the $\mathbf{x}_t$. We also assume that the channel between the SN and RN is h_r and h_d is the channel between the RN and DN. Let us also assume that h_{r_1} is the channel between radar and relay and h_{d_1} is the channel between radar and DN. All the

channels are assumed to be of single tap ones. Let us define $\mathbf{r}_r^1 \in \mathbb{C}^{L\times 1}$ as the received data at the RN. Therefore, the corresponding relay received signal is expressed as

$$\mathbf{r}_r^1 = h_r \mathbf{x}_t^o + h_{r_1}\mathbf{c}_r^o + \mathbf{n}_1, \tag{2}$$

where $\mathbf{x}_t^o \in \mathbf{C}^{L\times 1}$, $\mathbf{c}_r^o \in \mathbf{C}^{L\times 1}$ are the vectors consisting of the odd-positioned data of $\mathbf{x}_t$ and $\mathbf{c}_r$, respectively. Also, $\mathbf{n}_1 \in \mathbf{C}^{L\times 1}$ is the additive white Gaussian noise (AWGN) at the RN with power spectral density σ_1^2 for each element. Each element of $\mathbf{r}_r^1$ will be amplified by a scalar factor α_i for $i = 1, 2, \ldots, L$ and then transmitted. Assume that $\mathbf{A}_r = diag[\alpha_1, \alpha_2, \ldots, \alpha_L]$ is the relay amplify coefficient matrix at the RN. Hence, the transmitted data vector from the RN is $\mathbf{r}_r^t \in \mathbb{C}^{L\times L} = \mathbf{A}_r\mathbf{r}_r^1$. Each element of $\mathbf{r}_r^t$ is the even element of $\mathbf{r}_r$. Similarly, the received data $\mathbf{r}_d \in \mathbb{C}^{L\times 1}$ at the DN is expressed as

$$\begin{aligned}\mathbf{r}_d &= h_d\mathbf{r}_r^t + h_{d_1}\mathbf{c}_r^e + \mathbf{n}_2 \\ &= h_d h_r \mathbf{A}_r\mathbf{x}_t^o + \left[h_d h_{r_1}\mathbf{A}_r\mathbf{c}_r^o + \mathbf{A}_r\mathbf{n}_1 + h_{d_1}\mathbf{c}_r^e\right] + \mathbf{n}_2,\end{aligned} \tag{3}$$

where $\mathbf{n}_2$ is the AWGN at the DN with power spectral density σ_2^2 for each element and $\mathbf{c}_r^e \in \mathbb{C}^{L\times 1}$ is the collection of all even-positioned elements of $\mathbf{c}_r$.

III. COST FUNCTION DEVELOPMENT

In this RadRCom system, we consider both radar centric and relay-centric designs separately with the respective cost function (CF).

1) CF FOR RADAR-CENTRIC DESIGN

In the first case, we will maximize the received average SINR at the radar receiver (Rx). It will ensure certain QoS parameters i.e MSE, power level etc. to be maintained at the communication ends as well. Let us assume that the radar transmit sequence will have average power of $\|\mathbf{c}_r\|^2 = P_c$. The average SINR at the radar Rx with the knowledge of channel gains can be expressed as

$$\gamma = \frac{|h_c|^2\|\mathbf{c}_r\|^2}{I + K\sigma_r^2}, \tag{4}$$

where I is the average interference at the radar and is defined as

$$\begin{aligned}I &= \sigma_x^2|h_1|^2L + |h_2|^2\|\mathbf{r}_r^t\|^2 \\ &= \sigma_x^2|h_1|^2L + |h_2|^2\times \\ &\quad\left[\left[|h_r|^2\sigma_x^2 + \sigma_1^2\right]\sum_{l=1}^{L}\alpha_l^2 + |h_{r_1}|^2\|\sum_{l=1}^{L}\alpha_l^2\mathbf{c}_r^o(l)\|^2\right].\end{aligned} \tag{5}$$

2) CF FOR RELAY CENTRIC DESIGN

In the second case, we will minimize the MSE of the detected data at the DN. As the channels do not change during the KT_c time, let us assume that the equalizer matrix is $\mathbf{W}_d = diag[w_1\ w_2 \ldots w_L]$, which will be diagonal because each element of $\mathbf{r}_d$ is uncorrelated. Thus, the MSE at the DN for the l^{th} received data for $l = 1, 2, \ldots, L$ can be calculated as

$$\begin{aligned}MSE_d^l &= \mathbb{E}\|\mathbf{x}_t^o(l) - w_l\mathbf{r}_d(l)\|^2 \\ &= \sigma_x^2 - w_l^*h_d^*h_r^*\sigma_x^2 + |w_l h_d h_r|^2\sigma_x^2 - w_l h_d h_r\sigma_x^2 \\ &\quad + \alpha_l h_d h_{r_1} c(2l)h_{d_1}^* c^*(2l+1) + \alpha_l^2|h_d h_{r_1} c(2l)|^2 \\ &\quad + \alpha_l h_{d_1} c(2l+1)h_d^* h_{r_1}^* c(2l) + |h_{d_1} c(2l+1)|^2 \\ &\quad + \sigma_2^2 + \alpha_l^2\sigma_1^2.\end{aligned} \tag{6}$$

Hence, the total MSE is defined as

$$\rho \triangleq \sum_{l=1}^{L} MSE_d^l. \tag{7}$$

Moreover, both optimization processes are inherently governed by specific constraints. One crucial constraint involves an energy limit on the radar code, represented as $\|\mathbf{c}_r\|^2 \le P_c$, where P_c denotes the maximum transmit energy for the radar code. Beyond the energy constraint, a similarity constraint is enforced, aligning the radar code with a reference code of unit energy, denoted as $\mathbf{c}_0$. This similarity constraint guarantees a specified resemblance between the radar code and the reference code with unit energy [4], [34]. For radar-centric scenarios, our main objective is to maximize the SINR of the radar. This optimization is carried out while simultaneously restricting the MSE of communication to establish a balanced trade-off between the two objectives. Likewise, in relay-centric optimization, the SINR at the radar receiver is mandated as a constraint, along with constraints on relay power. The detailed optimization statement is provided in the following section.

IV. OPTIMIZATION METHODS

In this section, we will focus on two optimization statements, i.e., radar-centric and relay-centric, separately.

A. RADAR CENTRIC OPTIMIZATION

The optimization framework for the radar centric aspect can be formulated as follows [4], [34]

$$\begin{aligned}\left[\boldsymbol{\alpha}^{opt}, \boldsymbol{c}_r^{opt}, \mathbf{w}^{opt}\right] = \underset{\boldsymbol{\alpha},\mathbf{c}_r,\mathbf{w}}{\arg}\ &\max\ \gamma, \\ \text{s.t}\ \ &(a)\ \ \rho \ge \rho_{th} \\ &(b)\|\mathbf{c}_r\|^2 = P_c, \\ &(c)\|\mathbf{c}_r - \mathbf{c}_0\|^2 \le \epsilon,\end{aligned} \tag{8}$$

In addition to the energy constraint, a similarity constraint is imposed, aligning the radar code with a unit energy reference code, denoted as $\mathbf{c}_0$. The similarity constraint ensures a prescribed resemblance between the radar code and the reference code with unit energy [4], [34] and ϵ is a design parameter related to the error.

B. RELAY CENTRIC OPTIMIZATION

The optimization for the relay-centric aspect can be formulated as [34]

$$\begin{aligned}\left[\boldsymbol{\alpha}^{opt}, \boldsymbol{c}_r^{opt}, \mathbf{w}^{opt}\right] = \underset{\boldsymbol{\alpha}, \mathbf{c}_r, \mathbf{w}}{\arg\ \min}\ \rho,\\ \text{s.t}\ \ (a)\ \ \gamma \geq \gamma_{th}\\ (b)\|\mathbf{c}_r\|^2 = P_c\\ (c)\|\mathbf{c}_r - \mathbf{c}_0\|^2 \leq \epsilon\\ (d)\mathbb{E}\|\mathbf{r}_r^t\|^2 \leq P_r. \end{aligned} \tag{9}$$

where $\mathbb{E}\|\mathbf{r}_r^t\|^2$ can be expressed as

$$\mathbb{E}\|\mathbf{r}_r^t\|^2 = \left[|h_r|^2\sigma_x^2 + \sigma_1^2\right]\sum_{l=1}^{L}\alpha_l^2 + |h_{r_1}|^2\|\sum_{l=1}^{L}\alpha_l^2\mathbf{c}_r^o(l)\|^2. \tag{10}$$

Since we are formulating two distinct optimization statements, the decision not to opt for multi-objective optimization stems from a particular consideration. In multi-objective optimization, the challenge lies in finding a single decision vector that effectively balances the trade-offs among various objectives. Solutions that achieve an optimal trade-off, referred to as Pareto optimal solutions, represent decision vectors where improvement in one objective must necessarily come at the expense of another. Although [28] delves into the Pareto optimization problem within a dual-function radar communication framework, the exploration of this problem in the context of coexistence joint radar communication scenarios remains unaddressed. Furthermore, Pareto optimization in the coexistence scenario can be a future direction for our research work. Therefore, in line with other works in RadCom domain [34], we have chosen to focus separately on radar-centric and communication-centric optimization problems so that the decision is grounded in the acknowledgment that achieving optimal performance in one domain while preserving the performance of the other system is a delicate balancing act. For instance, in radar-centric optimization, our primary goal is to maximize the SINR at the radar while simultaneously constraining the MSE of communication to maintain a trade-off between the two. This deliberate separation allows us to navigate the intricate landscape of conflicting objectives, ensuring that the optimization efforts are tailored to the unique requirements and constraints of each subsystem.

C. ALGORITHM DESIGN

1) RADAR CENTRIC ALGORITHM

The optimization problem in (8) is non-convex with higher complexity with respect to the joint optimization variables. In the radar-centric cost function, we consider MSE of the communication system as a constraint due to coexisting radar and relay communication systems. However, we propose an iterative method in which a two-step approach is adopted. In the first part, we consider the nonlinear constraints (b), (c) only to find intermediate optimum value of $\mathbf{c}_r$ keeping other two variables initialized. The first step optimization problem can be stated as

$$\begin{aligned}\left[\boldsymbol{c}_r^{opt}\right] = \underset{\boldsymbol{c}_r}{\arg\max}\ \gamma,\\ (b)\|\mathbf{c}_r\|^2 = P_c\\ (c)\|\mathbf{c}_r - \mathbf{c}_0\|^2 \leq \epsilon. \end{aligned} \tag{11}$$

The cost function is not convex in nature with respect to $\mathbf{c}_r$. So, we adopted a sequential quadratic programming (SQP) algorithm to solve it [35].

After solving (11), we obtain an intermediate optimal value of $\mathbf{c}_r$ and use it for the next step. We update the $\mathbf{c}_r$ value into the other constraint, i.e, MSE along with cost function and solve for $\boldsymbol{\alpha}$ and $\mathbf{w}$. Therefore, the step-two problem statement can be stated as

$$\begin{aligned}\left[\boldsymbol{\alpha}^{opt}, \mathbf{w}^{opt}\right] = \underset{\boldsymbol{\alpha}, \mathbf{w}}{\arg\max}\ \gamma,\\ \text{s.t}\ \ (a)\ \ \rho \geq \rho_{th}. \end{aligned} \tag{12}$$

Intermediate solutions for $\boldsymbol{\alpha}$ and $\mathbf{w}$ are used again in (11) and the iterations continue till an exit criterion is met. The overall steps are summarized in Algorithm-1.

Algorithm 1 Proposed Radar Centric Optimization

Input: $h_c, k, L, P_c, P_r, \epsilon, \sigma_r^2$
Output: $\hat{c}_{r_{opt}}, \hat{\alpha}_{opt}, \hat{w}_{opt}$
Part-1 : Radar Waveform Optimization.
for $i = 1 : k$, **do:**
  Initialize the value c_r^e, c_r^o, α
    If $(\|\mathbf{c}_r\|^2 = P_c\ \&\ \|\mathbf{c}_r - \mathbf{c}_0\|^2 \leq \epsilon)$
      Obtain $\mathbf{c}_r$ using SQP
  break;
  End If
End For
optimized parameter:$\hat{c_r}, \alpha_{new}$
Update: $\gamma \leftarrow \hat{c_r} = \gamma_{new}, \rho \leftarrow \hat{c_r} = \rho_{new}$
Part-2 : Relay Power gain and Equalizer Optimization
For $j = 1 : L$, **do:**
  Initialize: $c_r \leftarrow \hat{c_r}, \alpha \leftarrow \alpha_{new}, w$
    If $(\rho_{new} \leq \rho_{th})$
      Obtain $\mathbf{w}, \alpha$ using SQP
  break;
  End If
End For
optimized parameter: $\hat{\alpha}, \hat{w}$
Store:$\hat{c}_{r_{opt}} = \hat{c_r}, \hat{\alpha}_{opt} = \hat{\alpha}, \hat{w}_{opt} = \hat{w}$

2) RELAY CENTRIC ALGORITHM

The relay-centric algorithm has been proposed separately from previous algorithm. Here $\mathbf{c}_r$ is split into two sets of variables, *i.e.* odd $(\mathbf{c}_r^o)$ and even $(\mathbf{c}_r^e)$ parts. So, this

optimization problem can be rewritten as

$$\begin{aligned}\left[\boldsymbol{\alpha}^{opt}, \mathbf{c}_r^{o^{opt}}, \mathbf{c}_r^{e^{opt}} \mathbf{w}^{opt}\right] = \underset{\boldsymbol{\alpha},\mathbf{c}_r,\mathbf{w}}{\arg\min}\ \rho,\\ \text{s.t } (a)\ \gamma \geq \gamma_{th}\\ (b)\|\mathbf{c}_r\|^2 = \| \mathbf{c}_r^o \|^2 + \| \mathbf{c}_r^e \|^2 = P_c\\ (c)\|\mathbf{c}_r^o - \mathbf{c}_0^o\|^2 + \|\mathbf{c}_r^e - \mathbf{c}_0^e\|^2 \leq \epsilon\\ (d)\mathbb{E}\|\mathbf{r}_r^t\|^2 \leq P_r. \end{aligned} \tag{13}$$

Solving the optimization problem presented above is challenging due to the non-convex nature of constraint (a) and the multi-variable structure of the objective function. The problem involves a matrix variable with a length of L^2 and three vector variables, each with a length of L, resulting in a total of $2L^2 + 5L$ real variables. To alleviate the complexity, a strategy is employed wherein the equalizer, originally represented as a matrix, is simplified to a diagonal matrix. While this approach offers a lower-cost solution, it comes at the expense of increased mean squared error (MSE). The new updated MSE is denoted as

$$MSE(\rho) \triangleq \mathbb{E}\|\mathbf{x}_t^o - \mathbf{W}_d \mathbf{r}_d\|^2, \tag{14}$$

where $\mathbf{W}_d = diag(\mathbf{w})$, $\mathbf{w}$=$[w_1, w_2, \ldots . w_L]^T$. Again it can be rewriten as

$$\begin{aligned} MSE(\rho) = L\sigma_x^2 - h_d h_r \sigma_x^2 \alpha^* \mathbf{w} - h_d^* h_r^* \sigma_x^2 \mathbf{w}^* \alpha + \sigma_2^2 \mathbf{w}^* \mathbf{w}\\ + |h_d h_r|^2 \sigma_x^2 \mathbf{w}^* \alpha \alpha^* \mathbf{w} + |h_d|^2 \sigma_1^2 \mathbf{w}^* \alpha \alpha^* \mathbf{w}\\ + |h_d h_{r_1}|^2 \mathbf{c_r^{o^*}} \mathbf{A_r^* W^* W A_r c_r^o}\\ + |h_{d_1}|^2 \mathbf{c_r^{e^*}} \mathbf{W^* W c_r^e} + h_d^* h_{r_1}^* h_{d_1} \mathbf{c_r^{o^*}} \mathbf{A_r^* W^* W c_r^e}\\ + h_d h_{r_1} h_{d_1}^* \mathbf{c_r^{e^*}} \mathbf{W^* W A_r^* c_r^o}. \end{aligned} \tag{15}$$

One way to further simplify the above cost function is by converting all the vectors into scalars and calculating MSE symbol-by-symbol as

$$\begin{aligned} MSE_l^d &= \mathbb{E}\|x_t^o(l) - w_l r_{d_1}(l)\|^2\\ &= \sigma_x^2 - w_l^* h_d^* h_r^* \alpha_l \sigma_x^2 - w_l h_d h_r \alpha_l \sigma_x^2 + |w_l h_d h_r|^2 \alpha_l^2 \sigma_x^2\\ &\quad + h_d h_{r_1} h_{d_1}^* c_r^e(l) c_r^{o^*}(l) \alpha_l |w_l|^2 + |w_l h_{d1} c_r^e(l)|^2\\ &\quad + |w_l|^2 \sigma_2^2 + h_d^* h_{r_1}^* h_{d_1} c_r^o(l) c_r^{e^*}(l) \alpha_l |w_l|^2\\ &\quad + |h_d h_{r_1} w_l c_r^o|^2 \alpha_l + |w_l h_d|^2 \alpha^2 \sigma_1^2. \end{aligned} \tag{16}$$

The total MSE is $\rho = \sum_{l=1}^{L} MSE_l^d$. Similarly, the constraints can be divided into scalar counterparts, and the optimization problem becomes

$$\begin{aligned}\left[\alpha_l^{opt}, c_r^{o^{opt}}, c_r^{e^{opt}}, w_l^{opt}\right] = \underset{\alpha_l, c_r^o, c_r^e, w_l}{\arg}\ MSE_l^d\\ \text{s.t } (a)\gamma \geq \gamma_{th}\\ (b)|c_r^o(l)|^2 + |c_r^e(l)|^2 = P_c/L\\ (c)|c_r^o(l) - c_0^o(l)|^2 \leq \epsilon'\\ (d)|c_r^e(l) - c_0^e(l)|^2 \leq \epsilon'\\ (e)\left[|h_r|^2 + \sigma_x^2\right]\alpha_l^2\\ + |h_{r_1}|^2 |c_r^o(l)|^2 \alpha_l^2 \leq P_r/L. \end{aligned} \tag{17}$$

Similar approaches have been adopted in solving (17) like the radar-centric case as summarized in Algorithm-1. The process is iterated L times. Additionally, in Algorithm-2, we have summarized the relay-centric algorithm.

Algorithm 2 Proposed Relay Centric Optimization

1) **Input:** $k, L, P_c, P_r, \epsilon', \sigma_r^2$
2) **Output:** $\hat{c_r}^{o^{opt}}, \hat{c_r}^{e^{opt}}, \hat{\alpha}_l^{opt}, \hat{w_l}^{opt}$
3) **Part-1: for** $i = 1 : k$, **do:**
4) **If** $(|c_r^o(l)|^2 + |c_r^e(l)|^2 = P_c/L, |c_r^o(l) - c_0^o(l)|^2 \leq \epsilon' |c_r^e(l) - c_0^e(l)|^2 \leq \epsilon', \gamma \geq \gamma_{th})$
Obtain $\mathbf{c}_r$ using SQP
5) **End If**;
End For;
6) optimized parameter:$\hat{c_r}^{o^{opt}}, \hat{c_r}^{e^{opt}}$
7) Update: $\gamma \leftarrow \hat{c_r} = \gamma_{new}, \rho \leftarrow \hat{c_r} = \rho_{new}$
8) **Part-2: For** $j = 1 : L$, **do:**
9) **If** $([|h_r|^2 + \sigma_x^2]\alpha_l^2 + |h_{r_1}|^2 |c_r^o(l)|^2 \alpha_l^2 \leq P_r/L)$
Obtain $\hat{\alpha}_l^{opt}, \hat{w_l}^{opt}$ using SQP
10) **End If**;
End For;
11) optimized parameter: $\hat{\alpha}_l^{opt}, \hat{w_l}^{opt}$

FIGURE 3 comprehensively illustrates the flowchart outlining our proposed methodology for both radar-centric and relay-centric scenarios. This flowchart shows both the algorithms. The left side illustrates the radar-centric algorithm and the right one demonstrates the relay-centric part.

V. PERFORMANCE ANALYSIS

A. RADAR DETECTION ANALYSIS

Radar optimization is followed by radar detection which is an integral part at the radar end. We analyze the radar detection performance here. From equation (1), we can rewrite the radar data model as,

$$\begin{aligned}\mathbf{y}_r &= h_c \mathbf{c}_r + h_1 \mathbf{x}_t + h_2 \mathbf{r}_r + \mathbf{n}_r\\ &\triangleq h_c \mathbf{c}_r + \mathbf{p}_r + \mathbf{n}_r, \end{aligned} \tag{18}$$

where $\mathbf{p}_r \in \mathbb{C}^{K \times K}$ is the interference for the radar system coming from the communication source and relay. It can be simplified as

$$\begin{aligned}\mathbf{p}_r &= h_1 \mathbf{x}_t + h_2 \mathbf{r}_r\\ &= h_1 \mathbf{x}_t + h_2 \mathbf{I}_e \left[h_r \mathbf{A}_r \mathbf{x}_t^0 + h_{r1} \mathbf{A}_r \mathbf{c}_r^o + \mathbf{A}_r \mathbf{n}_1\right], \end{aligned} \tag{19}$$

where $\mathbf{I}_e \in \mathbb{R}^{K \times L}$ is an identity matrix with even rows having all-zero vector. Similarly, we define that $\mathbf{I}_o \in \mathbb{R}^{K \times L}$

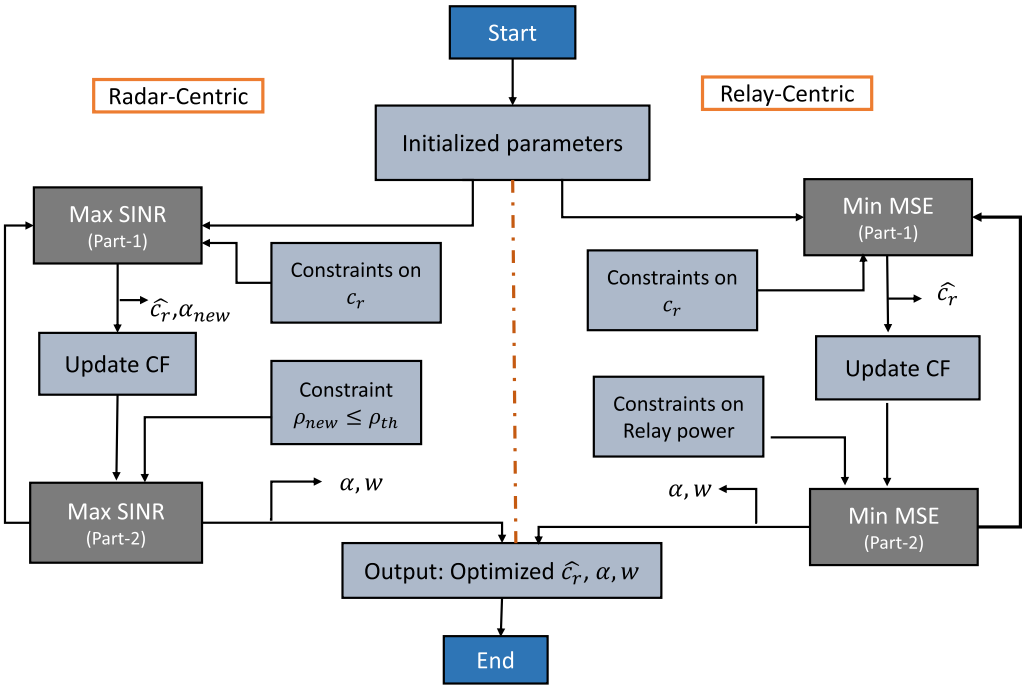

FIGURE 3. Flowchart of optimization of the RadRCom system for design parameter estimation.

is an identity matrix with odd rows having all-zero vectors. Therefore, the mean of the interference plus noise ($\mathbf{n}'_r \triangleq \mathbf{p}_r + \mathbf{n}_r$) is computed as $\mu_r \triangleq h_2 h_{r1} \mathbf{I}_e \mathbf{A}_r \mathbf{c}_r^o$. Effective noise vector $\mathbf{n}'_r$ has non-equal mean at each position. After subtracting μ_r from $\mathbf{y}_r$, the modified received vector at the radar is written as

$$\mathbf{y}'_r = h_c \mathbf{c}_r + \mathbf{n}'_r - \mu_r. \tag{20}$$

The final effective noise ($\mathbf{n}'_r - \mu_r$) has zero mean and its covariance matrix can be computed as

$$\begin{aligned}\mathbf{C}_r = \sigma_r^2 \mathbf{I} + \|h_1\|^2 \sigma_x^2 \mathbf{I}_e \mathbf{I}_e^T + \|h_2\|^2 \|h_r\|^2 \sigma_x^2 \mathbf{I}_e \mathbf{A}_r \mathbf{A}_r^* \mathbf{I}_e^T \\ + \|h_2\|^2 \mathbf{I}_e \mathbf{A}_r \mathbf{A}_r^* \mathbf{I}_e^T.\end{aligned} \tag{21}$$

It is observed that $\mathbf{C}_r$ is a diagonal matrix having unequal diagonal elements. The effective noise vector is not Gaussian, though an optimal Neyman Pearson (NP) detector, which may be complex enough, can be designed. However, we consider a sub-optimal one for performance analysis purposes. We compute an inner product between $\mathbf{c}_r$ and $\mathbf{y}'_r$ with some normalization factor as $z_r = \dfrac{\mathbf{c}_r^* \mathbf{y}'_r}{h_c \sqrt{\mathbf{c}_r^* \mathbf{C}_r \mathbf{c}_r}}$. The noise quantity $n_e = \dfrac{\mathbf{c}_r^* (\mathbf{n}' - \mu_r)}{h_c \sqrt{\mathbf{c}_r^* \mathbf{C}_r \mathbf{c}_r}}$ is a normalized sum of zero mean non-identical random variables. If $K \to \infty$ (or large enough), we can apply the central limit theorem (CLT) with the Lyapunov condition and conclude that n_e is Gaussian with zero mean and unit variance. With this assumption, a binary hypothesis is built as [36]

$$\begin{aligned} H_0 &: \ z_r = n_e \\ H_1 &: \ z_r = \frac{\|\mathbf{c}_r\|}{h_c \sqrt{\mathbf{c}_r^* \mathbf{C}_r \mathbf{c}_r}} + n_e. \end{aligned} \tag{22}$$

Let us assume that α_f is the probability of false alarm (PFA). Therefore, the probability of detection (P_D) can be found for a given PFA α_{pfa} as follows [36]

$$P_D = Q\left(Q^{-1}\left(\alpha_{pfa}\right) - \sqrt{\frac{\|\mathbf{c}_r\|^2}{\|h_c\|^2 \mathbf{c}_r^* \mathbf{C}_r \mathbf{c}_r}} \right). \tag{23}$$

B. SER ANALYSIS AT DN FOR RADAR CENTRIC DESIGN

The received signal at the DN is represented in (3). The estimated data is represented as $\hat{\mathbf{x}}_t^o = \mathbf{W}_d \mathbf{r}_d$. If P_e^l is the probability of error for the l^{th} data, then the total probability of error will be as follows [6]

$$P_e = \frac{1}{L} \sum_{l=1}^{L} P_e^l. \tag{24}$$

We assume here that $L = K/2$, i.e the radar signal length is even. We now calculate P_e^l. The interference and noise at the $(2l-1)^{th}$ odd-position after the equalization is $n_d^l \triangleq (\mathbf{w}_d^l)^* \left[h_d h_{r_1} \mathbf{A}_r \mathbf{c}_r^o + \mathbf{A}_r \mathbf{n}_1 + h_{d_1} \mathbf{c}_r^e + \mathbf{n}_2 \right]$, where $\mathbf{w}_d^l$ is a vector of zeros except w^l coefficient at the l^{th} position. Note that n_d^l is not Gaussian in general, but will be so for a fixed $\mathbf{c}_r$. We assume that the radar will have a fixed set of codes in a codebook $\mathbf{C}_r \in \mathbb{C}^{K \times M_c}$ and will use it with a probability of $p_m \triangleq P_r(\mathbf{c}_r = \mathbf{C}_r[m])$, where M_c is the total number of codes, $\mathbf{C}_r[m]$ is the m^{th} column/code. Furthermore, the P_e^l in (24) can be expressed as follows

$$P_e^l = \mathbb{E}_{\mathbf{h}} \left[P_{e|\mathbf{h}}^l \right], \tag{25}$$

where $P_{e|\mathbf{h}}^l$ is the instantaneous probability of error at the DN for the given $\mathbf{C}_r[m]$ and $h_r, h_d, h_{r_1}, h_{d_1}$. For an M-quadrature

TABLE 1. Simulation parameters.

Parameter Name	Value
Carrier Frequency	5.9 GHz
Bandwidth	5 MHZ
Communication Signal	QPSK
Coverage radius	200 m
ϵ	0.01 (Default)
Radar object	Single
Speed of DN, radar object	0-30 kmph
Radar power	20 dBm (Default)
Code length (K)	32 (Default)
Communication Tx, RN power	20 dBm (Default)
Optimization iteration limit	500
P_c	20 dBm
P_r	15 dBm

amplitude modulation (M-QAM) system, the $P^l_{e|\mathbf{h}}$ at the DN can be calculated as [6]

$$P^l_{e|\mathbf{h}} \leq 4Q\left(\sqrt{\frac{3\xi_x}{(M-1)\sigma_e^2}}\right) \triangleq 2\exp\left[-\frac{3\xi_x}{2(M-1)\sigma_e^2}\right], \quad (26)$$

where ξ_x is denoted as $\mathbf{w}_d|h_d|^2|h_r|^2\sigma_x^2(\mathbf{A}_r\mathbf{A}_r^*)\mathbf{w}_d^*$ and the interference-noise covariance is denoted as $\sigma_e^2 = \mathbf{w}_d(|h_d|^2|h_{r1}|^2\mathbf{P}^o_{eq} + h_{d1}|^2\mathbf{C}^e_{eq} + \mathbf{Q}^e_{eq})\mathbf{w}_d^*$, where $\mathbf{P}^o_{eq} = \mathbf{A}_r\mathbf{c}_r^0\mathbf{c}_r^{0*}\mathbf{A}_r^*$ and $\mathbf{c}^e_{eq} = \mathbf{c}^e_r\mathbf{c}^{eo}_r, \mathbf{Q}^e_{eq} = \sigma_1^2\mathbf{A}_r\mathbf{A}_r^* + \sigma_2^2$. We consider that all the channels are zero-mean Gaussian distribution random variables. We have normalized the variance. Hence, the distributions of $|h_d|^2$, $|h_{d1}|^2$, $|h_r|^2$, $|h_{r1}|^2$ become Chi-squared distribution with two degrees of freedom. Let us assume that $\|h_r\|^2 = Z_1$, $\|h_{r1}\|^2 = Z_2$, $\|h_{d1}\|^2 = Z_3$, $\|h_d\|^2 = Z_4$ to compute the integration. Now, all of the channels are assumed to be independent of one another. Therefore, we integrate each variable independently while holding all other variables fixed to solve the equation (27), as shown at the bottom of the next page. We start from variable Z_1 with limit 0 to ∞ in (28), as shown at the bottom of the next page, and move on for other variables for integration. Integration with Z_1 is computed in (28). Following integration with Z_2, Z_3, Z_4, we obtain the final expression for P^l_e given in equation (29), as shown at the bottom of the next page.

Note on Future Challenges: RadRCom systems encounter several open challenges that demand focused research and innovation to ensure efficient relay communication. Spectrum allocation emerges as a critical concern with the escalating demand for radar applications, potentially leading to congestion and interference. The adoption of OFDM waveforms presents both opportunities and challenges in the context of RadRCom topology. Another key challenge is the Doppler tolerance. RadRcom system can also be extended to mmWave/THz communication with Beamforming and adaptation. Extension to MIMO for this proposed topology is also another future scope of work.

VI. NUMERICAL RESULTS

In this section, simulation results are presented to verify the proposed RadRCom method. The performances of the radar system and communication system are further illustrated with BER and MSE as the key QoS parameters. We use BER in place of SER during the numerical section as they are linearly related for uncoded system at higher SNR. Radar detection is also accomplished in this setup. This section is sub-categorized into two parts. In the first part, the performance of radar optimization will be given. In the next part, we will show the simulation results of the proposed algorithm on relay optimization.

A. SIMULATION BASED ON RADAR CENTRIC DESIGN

1) BER, MSE AND WAVEFORM DESIGN PERFORMANCE

In this part, we present simulation results that show how the maximization of SINR of the radar centric optimization affects the communication system. We obtain the optimized values of design parameters from radar centric algorithm and demonstrate the performance of the communication DN. Our main objective of this simulation process is to find out the effect of a radar system on communication using radar centric optimization. As previously discussed, we are assuming time-synchronization of the co-located single-antenna radar system and single antenna communication system. In the case of radar centric problem, our objective is to maximize the radar SINR, where communication data is the interference.

For this simulation setup, we consider a single antenna V2X scenario without the exact air-interface protocol [37]. We reiterate that this is a proof of concept and can be extended to any specific standard as per needs. The application scenario is restricted within a short range (within 200 m) radar detection with the radio frequency of 5.9 GHz. We have considered quadrature phase shift key (QPSK) constellation for the communication system and a flat-fading channel with independent and identically distributed Rayleigh fading, as the distance is short with low BW of 5 MHz [27], [37]. The default simulation parameters are given in Table-1. In addition, the reference radar waveform has a default length of $K = 32$ normalized to unit gain [38] unless specified.

Radar Waveform: In this setup, we consider the optimized radar waveform generation under the RadRCom scenario with the error limit as $\epsilon = 0.01, 0.001$. The comparison between the reference radar waveform and the optimized one is given in FIGURE 4 and FIGURE 5. In both the cases, we consider a randomly generated waveform to prove the efficiency of the proposed RadRCom. From both figures, it can be noted that the optimized waveform closely follows the reference one using the proposed Algorithm-1 framework. FIGURE 6 shows the waveform's MSE vs. various values of ϵ. Here, the MSE refers to error difference between the reference waveform and the one obtained from the proposed algorithm. We observe that with the decrease of ϵ, the MSE value also decreases. We have shown the MSE performance, keeping the radar power and relay power constant, which is

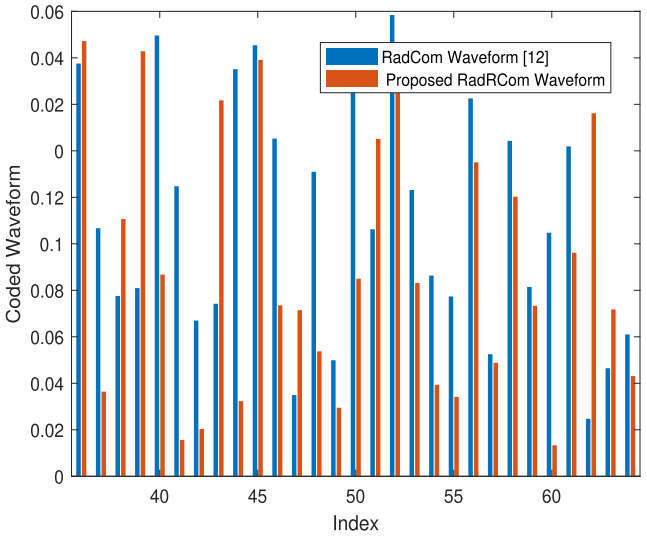

FIGURE 4. Comparison between reference radar waveform and optimized radar waveform with $\epsilon = 0.01$.

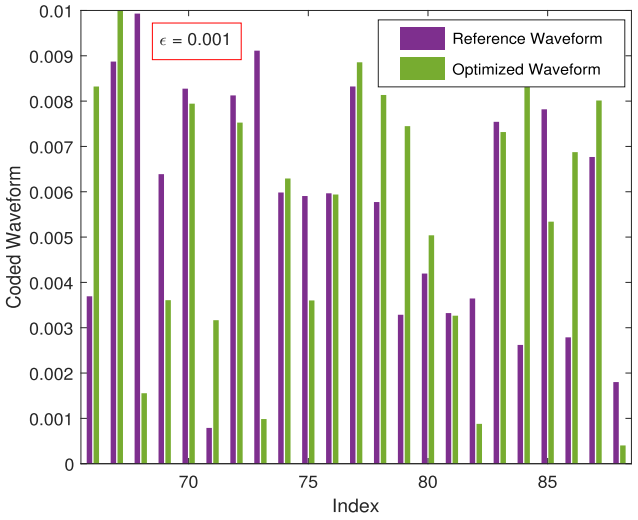

FIGURE 5. Comparison between reference radar waveform and optimized radar waveform with $\epsilon = 0.001$.

20 dBm. The performance is shown for three different Tx or SN powers. It can be observed that at 10 dBm Tx power, the radar waveform's MSE performance is better compared to the cases with increased Tx powers, i.e. 15 dBm, 20 dBm. This is because, when the Tx power decreases, it has lesser interference impact on the radar, which leads to the improved radar waveform error MSE performance.

MSE, BER Performance: The data detection performance at the final communication receiver (DN) is now demonstrated with respect to the radar centric optimization. QPSK data constellation is considered. It is assumed here that a reasonably good estimation of the channel is available, as this aspect is out of the scope of this work. In FIGURE 7, we plot the BER performance of the communication system at the DN with respect to the SINR, while keeping the radar

$$
\begin{aligned}
P_e^l &= 2\mathbb{E}\left[\exp\left[\frac{-3\mathbf{w}_d|h_d|^2|h_r|^2\sigma_x^2(\mathbf{A}_r\mathbf{A}_r^*)\mathbf{w}_d^*}{2(M-1)\mathbf{w}_d(|h_d|^2|h_{r1}|^2\mathbf{P}_{eq}^o + h_{d1}|^2\mathbf{C}_{eq}^e + \mathbf{Q}_{eq}^e)\mathbf{w}_d^*}\right]\right] \\
&= 2\int_{|h_d|^2}\int_{|h_{d1}|^2}\int_{|h_{r1}|^2}\int_{|h_r|^2}\exp -\frac{3}{2}\left[\frac{\mathbf{w}_d|h_d|^2|h_r|^2\sigma_x^2(\mathbf{A}_r\mathbf{A}_r^*)\mathbf{w}_d^*}{(M-1)\mathbf{w}_d(|h_d|^2|h_{r1}|^2\mathbf{P}_{eq}^o + h_{d1}|^2\mathbf{C}_{eq}^e + \mathbf{Q}_{eq}^e)\mathbf{w}_d^*}\right]\mathbf{p}(Z)\ \ d|h_r|^2\, d|h_{r1}|^2\, d|h_{d1}|^2\, d|h_d|^2 \\
&= 2\int_{Z_4}\int_{Z_3}\int_{Z_2}\int_{Z_1}\exp -\frac{3}{2}\left[\frac{\mathbf{w}_d Z_4 Z_1\sigma_x^2(\mathbf{A}_r\mathbf{A}_r^*)\mathbf{w}_d^*}{(M-1)\mathbf{w}_d(Z_4Z_2\mathbf{P}_{eq}^o + Z_3\mathbf{C}_{eq}^e + \mathbf{Q}_{eq}^e)\mathbf{w}_d^*}\right]\mathbf{p}(Z_4,Z_3,Z_2,Z_1)\ \ dZ_1\, d\, Z_2\, d\, Z_3\, d\, Z_4. \qquad (27)
\end{aligned}
$$

$$
\begin{aligned}
P_e^l(Z_1) &= \int_0^\infty \exp -\frac{3}{2}\left[\frac{\mathbf{w}_d Z_4 Z_1\sigma_x^2(\mathbf{A}_r\mathbf{A}_r^*)\mathbf{w}_d^*}{(M-1)\mathbf{w}_d(Z_4Z_2\mathbf{P}_{eq}^o + Z_3\mathbf{C}_{eq}^e + \mathbf{Q}_{eq}^e)\mathbf{w}_d^*}\right]\mathbf{p}(Z_1)\ \ dZ_1 \\
&= 2\frac{(M-1)[\mathbf{w}_d Z_4 Z_2\mathbf{P}_{eq}^o\mathbf{w}_d^* + \mathbf{w}_d Z_3\mathbf{c}_{eq}^e\mathbf{w}_d^* + \mathbf{w}_d Q_{eq}^e\mathbf{w}_d^*]}{-3\mathbf{w}_d Z_4\sigma_x^2(\mathbf{A}_r\mathbf{A}_r^*)\mathbf{w}_d^* + (M-1)[\mathbf{w}_d Z_4 Z_2\mathbf{P}_{eq}^o\mathbf{w}_d^* + \mathbf{w}_d\mathbf{Z}_3 c_{eq}^e\mathbf{w}_d^* + \mathbf{w}_d Q_{eq}^e)\mathbf{w}_d^*]} \\
&= \beta_1. \qquad (28)
\end{aligned}
$$

$$
\begin{aligned}
P_e^l &= \mathbb{E}_{\mathbf{h}}\left[P_{e|\mathbf{h}}^l\right] \\
&= \frac{1}{2}\left[6\sigma_x^2\mathbf{w}_d(\mathbf{A}_r\mathbf{A}_r^*)\mathbf{w}_d^*(M-1)\mathbf{w}_d Q_{eq}^e\mathbf{w}_d^* + \mathbf{w}_d Q_{eq}^e\mathbf{w}_d^* - 3(M-1)\mathbf{w}_d P_{eq}^O\mathbf{w}_d^* + 4(M-1)^2\mathbf{w}_d c_{eq}^e\mathbf{w}_d^*\mathbf{w}_d P_{eq}^O\mathbf{w}_d^*\right] \\
&= \frac{1}{2}(M-1)\left[6\sigma_x^2\mathbf{w}_d(\mathbf{A}_r\mathbf{A}_r^*)\mathbf{w}_d^*\mathbf{w}_d Q_{eq}^e\mathbf{w}_d^* + \mathbf{w}_d Q_{eq}^e\mathbf{w}_d^* - 3\mathbf{w}_d P_{eq}^0\mathbf{w}_d^* + 4(M-1)\mathbf{w}_d c_{eq}^e\mathbf{w}_d^*\mathbf{w}_d P_{eq}^O\mathbf{w}_d^*\right]. \qquad (29)
\end{aligned}
$$

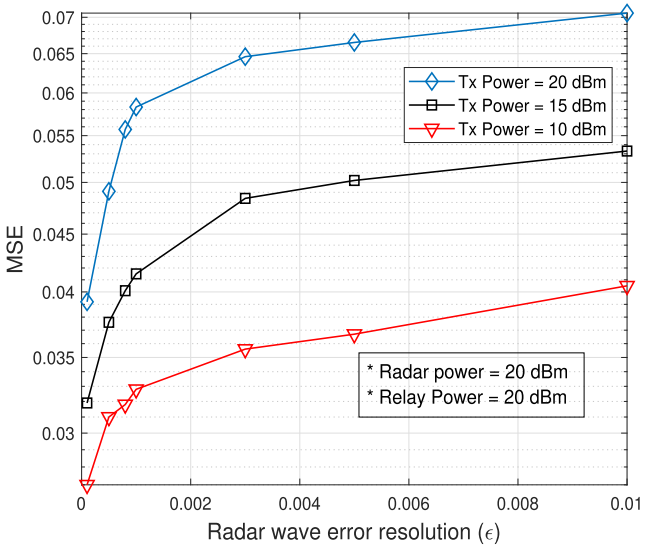

FIGURE 6. Comparison between reference radar waveform and optimized radar waveform with ϵ values.

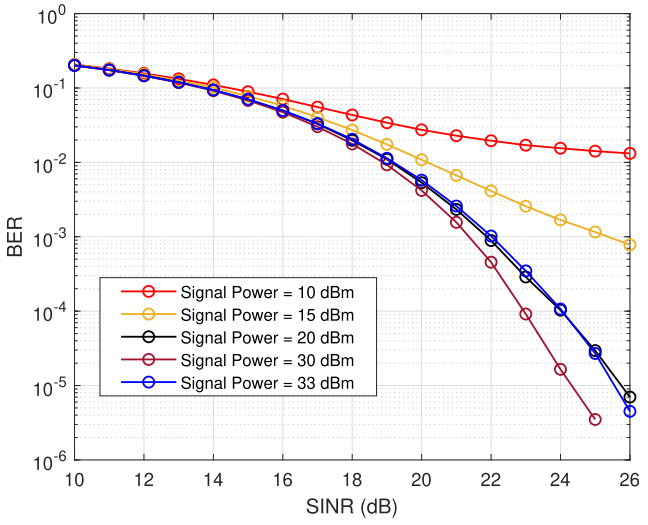

FIGURE 7. Performance evaluation of BER vs. SINR at the DN, when radar signal power is 30 dBm.

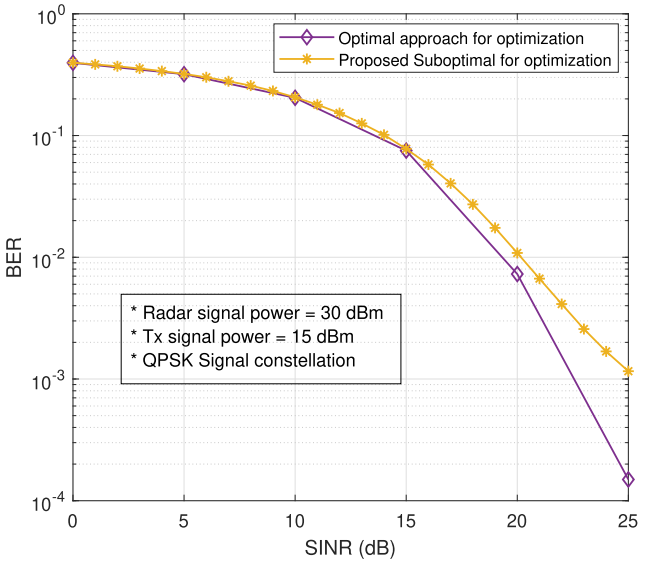

FIGURE 8. Performance evaluation of BER vs. SINR at the DN with the original optimization problem vs. the proposed sub-optimum approaches.

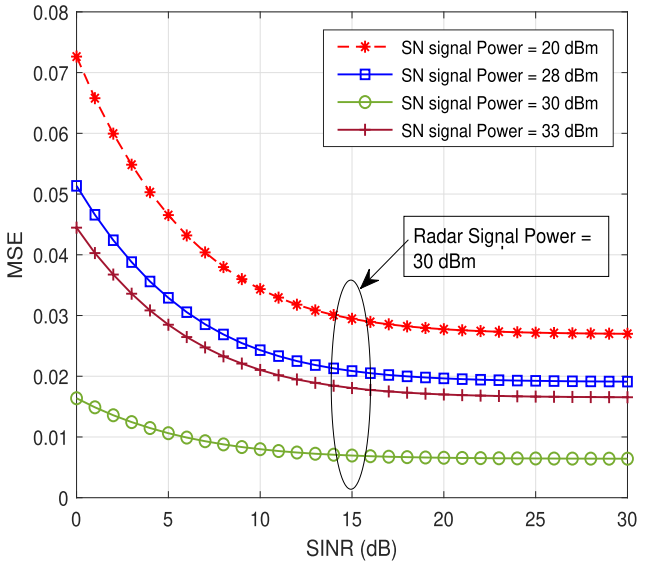

FIGURE 9. Performance evaluation of MSE vs. SINR at the DN, when radar signal power is fixed at 30 dBm.

transmit power constant at 30 dBm. We observe that when the communication transmit power at SN is reduced, within the range of 10 dBm to 15 dBm, the BER performance at the DN becomes flat beyond certain SINR value. This is due to the fact that the RN and DN get affected by the high interference from the radar signal and the SN transmit is not enough to counter this radar interference, which leads to flattening of BER curve after an SINR value. Therefore, this part is interference dominated rather AWGN dominated. In addition, the BER performance starts improving beyond 15 dBm SN transmit power, which counters the interference effect at the RN and DN. However, in the RadRCom, we observe another interesting phenomenon. If the SN transmit power increases further beyond 30 dBm, we observe that the BER degrades at 33 dBm SN power. This is because, when the SN power increases, the optimization framework continues to try to minimize the SINR at the radar by reducing the $\boldsymbol{\alpha}$, i.e. RN power coefficients. This continues to make the RN-DN link weaker. Beyond a certain point, this weaker RN-DN link results in BER degradation even if the SN power increases. In the same setup as before, the MSE performance of the transmitted data is plotted with respect to the received SINR at the DN in FIGURE 9. It can be observed that when radar power is fixed, the interference power at the DN is countered with the increasing SN transmit power. This improves the data MSE at the DN. However, the MSE performance does not improve significantly beyond a certain SINR due to interference from radar power. We also observe a similar

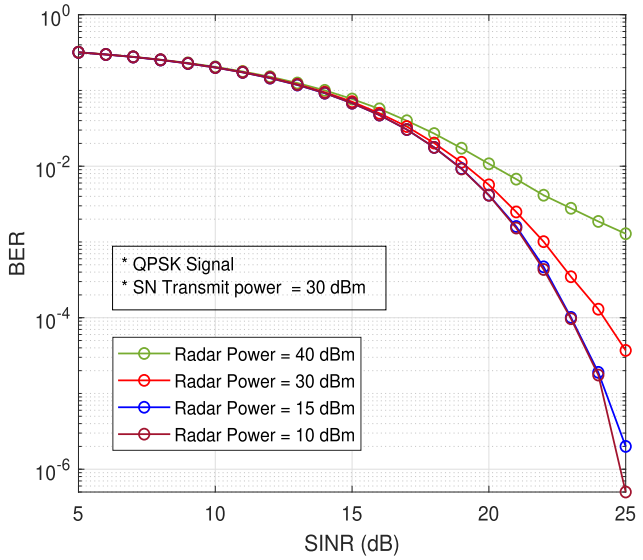

FIGURE 10. Performance evaluation of BER vs. SINR at DN, when SN transmit power is fixed at 30 dBm with various radar transmit powers.

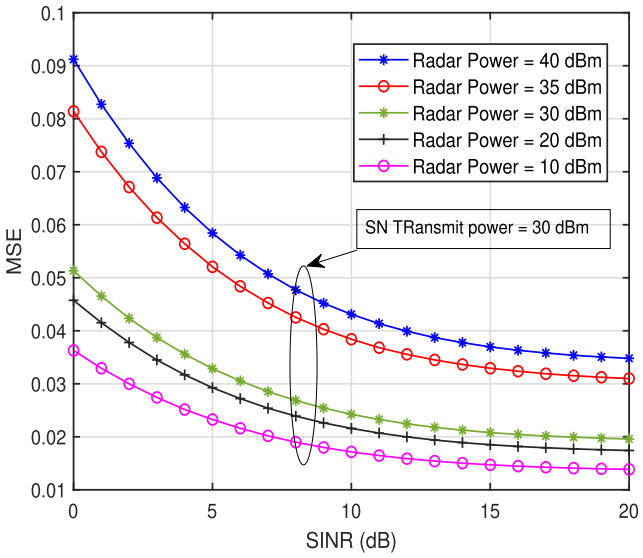

FIGURE 11. Performance evaluation of MSE vs. SINR at the DN, when SN transmit power is fixed as 30 dBm.

trend of MSE degradation beyond a certain level of SN power increase. In sync with the BER case, we also observe the MSE degradation at SN power of 33 dBm, while it improves till SN power of 30 dBm.

In this experiment setup, we now consider the SN transmit power a constant at 30 dBm, while we vary the radar transmit power in order to monitor the BER and MSE performance. FIGURE 10 plots the BER vs. SINR at the DN. We observe that as the radar power increases, the BER performance at the DN degrades. For example, we observe that the BER at the 40 dBm radar power is worse compared to the case with radar power of 30 dBm. The BER performance at DN is significantly enhanced when the radar power is at 10 dBm. This is because as the radar power increases, it causes more interference at the RN and DN, which impacts the BER performance. We also observe that the BER performance difference between radar power 15 dBm and 10 dBm is minimal. This is because these two radar powers may not create significant interference at the RN and DN under this experiment setup, as the SN power is enough to counter this interference. This also sets limit of differentiating interference at the communication system. FIGURE 8 plots the BER performance between the original optimization (8) and the proposed sub-optimal techniques. We observe that sub-optimal optimization has degraded BER performance, specially after the higher side of SNR. The MSE performance of the same system is shown in FIGURE 11. In this case, we observe that as the radar power increases, the MSE performance at DN degrades. The reason is as the radar power increases, the interference at the RN and DN increases, which degrades the MSE performance at the DN.

FIGURE 12 provides a comprehensive representation of the BER performance exhibited by the communication receiver under diverse M-QAM constellations. In this analysis, the radar power remains constant at 15 dBm, while the transmit signal power undergoes variation, as 15 dBm and 20 dBm. It shows the system's robustness and adaptability across different modulation schemes. Additionally, we simulate the BER under 16-QAM and 64-QAM constellations. This exploration not only enriches our understanding of the system's behavior but also underscores its versatility in accommodating various modulation configurations for optimal performance. FIGURE 13 illustrates the BER performance comparison between the existing RadCom and the proposed RadRCom systems. Given that relay-assisted radar communication, or RadRCom, constitutes a novel communication topology introduced in this study, there is a notable absence of prior research on this subject. Consequently, we conducted simulations assuming a poor link between the communication transmitter and receiver with a $8-10$ dB channel gain loss. For this specific scenario, simulations demonstrate an 8 dB gain when employing a relay between communication transmitter and receiver, i.e deploying the proposed RadRCom. Under the same scenario, we also assessed the MSE performance in this context, as depicted in FIGURE 14. Notably, the presence of a relay in the RadCom scenario resulted in improved performance, as evidenced by the MSE comparison.

2) RADAR DETECTION PERFORMANCE

In the previous section, we have shown how radar optimization affects the communication system in terms of BER and MSE plots. In this section, we evaluate the radar detection performance of the proposed method through several numerical simulations at the radar end. We carry out a performance evaluation of the proposed algorithms by resorting to standard Monte Carlo simulation. FIGURE 15 shows the region of convergence (ROC) curve of the P_D at the radar receiver. Here, we set the radar transmit power at

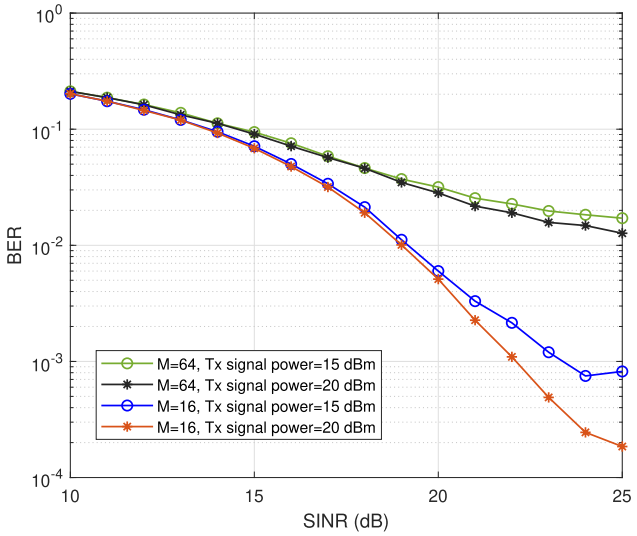

FIGURE 12. BER performance of communication receiver with different M-QAM constellations with 15 dBm radar power.

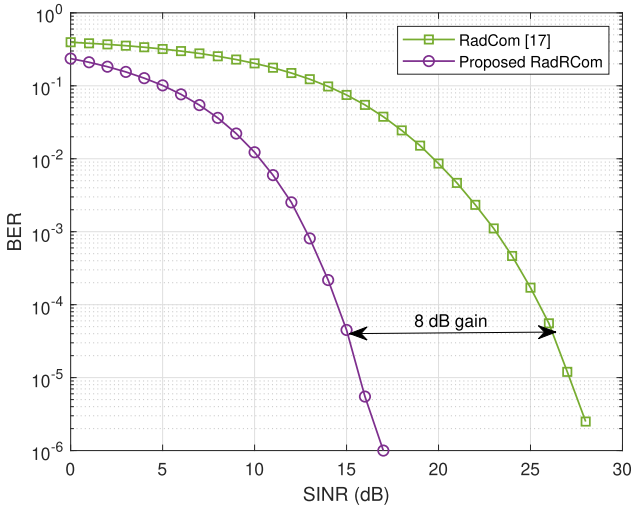

FIGURE 13. A comparative analysis of BER performance between the RadCom system and the proposed RadRCom system.

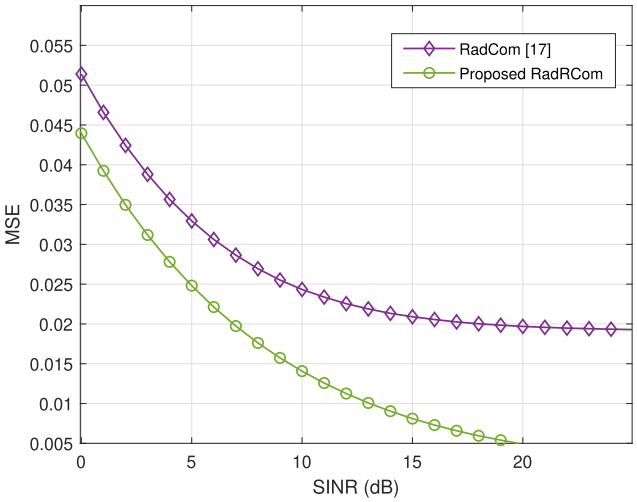

FIGURE 14. A comparison of MSE performance between the RadCom system and the proposed RadRCom system.

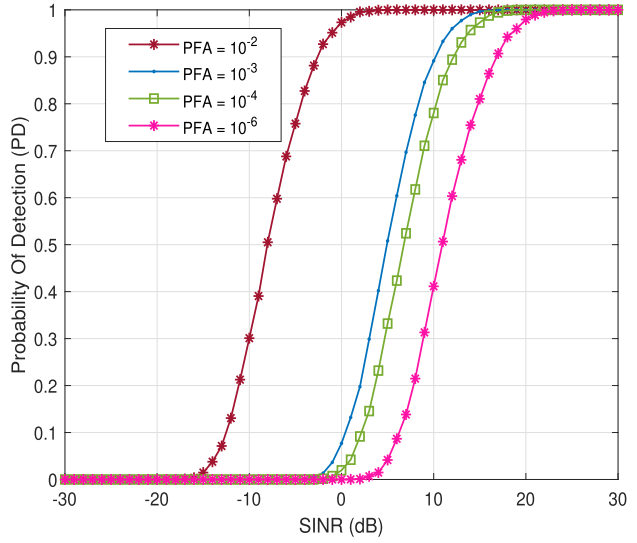

FIGURE 15. ROC curve for probability of detection vs. SINR at the radar receiver.

25 dBm and SN transmit power as 25 dBm. We now vary the target probability of a false alarm (PFA) from 10^{-2} to 10^{-6} and evaluate the P_D. As per the observations in the figure, we observe improved detection performance of radar waveform with the decrease in PFA. This is expected as per (23), as the P_D is inversely proportional to the PFA. In FIGURE 16, we plot the ROC performance with the SINR at the radar with different data length (L), which is $L = K/2$. The PFA is set at 10^{-2}. We observe that the detection probability improves with the increase in observable data length L. This is due to the fact that as the observable length increases, the noise part in (22) gets normalized with with larger data set, which reduces the effective variance of the noise leading to improvement in detection performance. FIGURE 17 plots the P_D vs. PFA for different SINR at the radar with fixed data length of $L = 64, K = 128$ and SN power of 20 dBm. The simulation result is obtained for SINR values of $[-20, -10, 10, 20]$ dB. We observe that P_D performance improves with the higher SINR at the radar. This is obvious due to the fact that as the radar SINR improves, the interference from the RN also decreases with the fixed SN power, leading to better detection performance at the radar. The probability of missed detection (PMD) is plotted in FIGURE 18. In this case, data length is fixed at $L = 64, K = 128$, SN power is kept at 20 dBm and SINR at the radar is varied from -20 dB to 20 dB. We observe that with the higher SINR, the probability of missed alarm decreases. This is due to the fact that as the SINR improves at the radar, it translates to the lower interference from the RN for fixed SN power.

B. SIMULATION BASED ON RELAY CENTRIC DESIGN

We now present the numerical results based on the relay centric optimization. FIGURE 19 plots the MSE performance

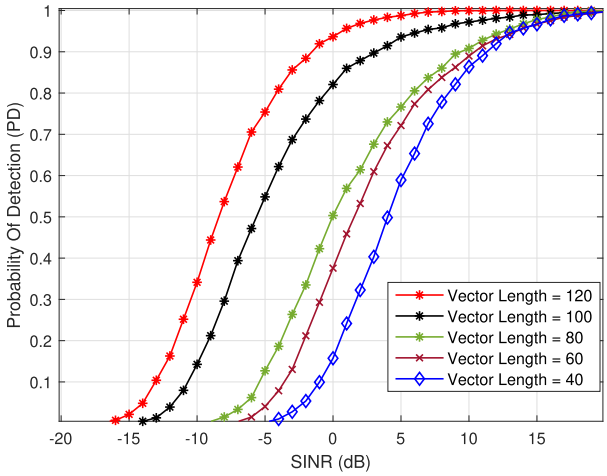

FIGURE 16. ROC curve for probability of detection vs. SINR at the radar with various observable radar data length *L*.

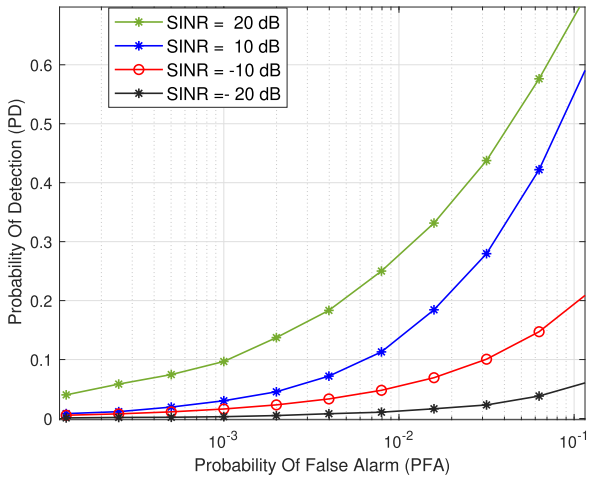

FIGURE 17. ROC curve for probability of detection vs. probability of false alarm.

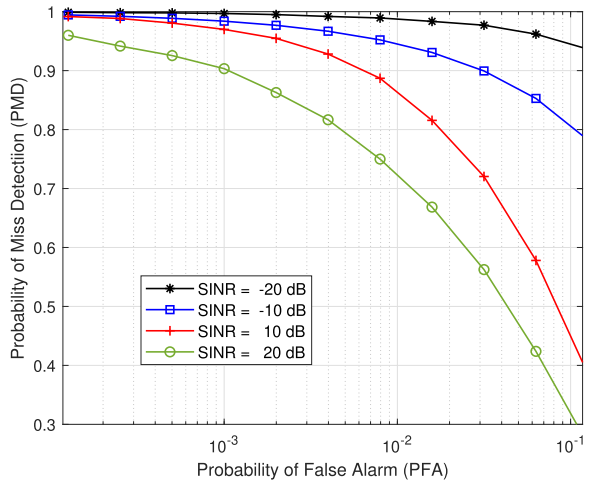

FIGURE 18. ROC plot for probability of detection vs. probability of false alarm at the radar SINR of 10 dB.

of data at the DN with SINR. We have kept the SN power at 25 dBm and also vary the radar power from [10 − 30] dBm. We observe that as the radar power increases, the MSE

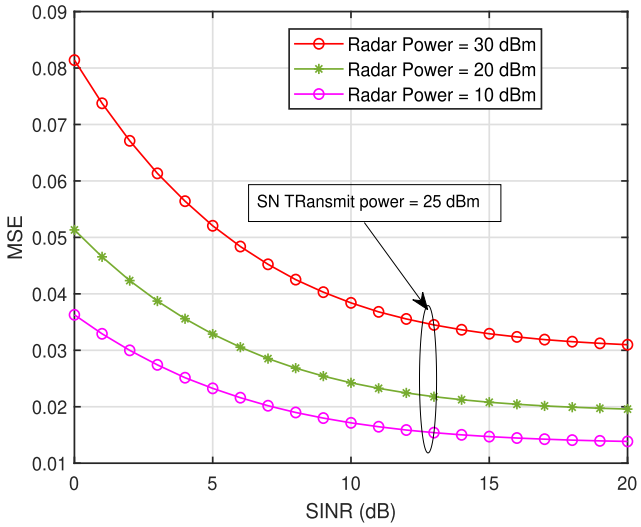

FIGURE 19. Performance evaluation of BER vs. SINR at the DN, when SN transmit power is fixed at 25 dBm.

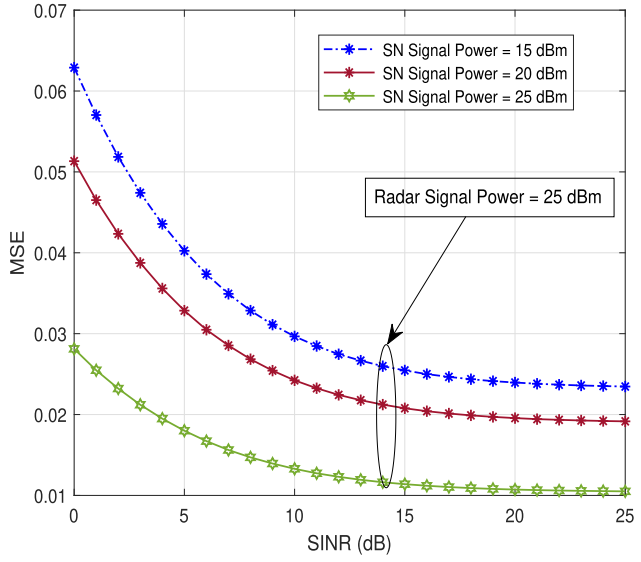

FIGURE 20. MSE Performance evaluation with respect to SINR at the DN, when radar transmit power is fixed at 25 dBm.

performance becomes poorer. This is due to the higher interference from the radar at the RN and DN. It is also noticed that even for higher SINR, the MSE performance becomes flat indicating that the radar interference dominates over the AWGN and the performance does not improve anymore. A similar trend is observed in FIGURE 20, where the data MSE at the DN is plotted for different SN power. It is observed that the MSE decreases with an increase in the SN power, till a point where the interference from the radar becomes dominant and from there onward, it doesn't change much due to interference from the radar. FIGURE 21 plots the BER vs. SINR at the DN. We keep the radar power at 25 dBm and vary the SN power from [10 − 25] dBm. We observe the improvement of BER with the increase in

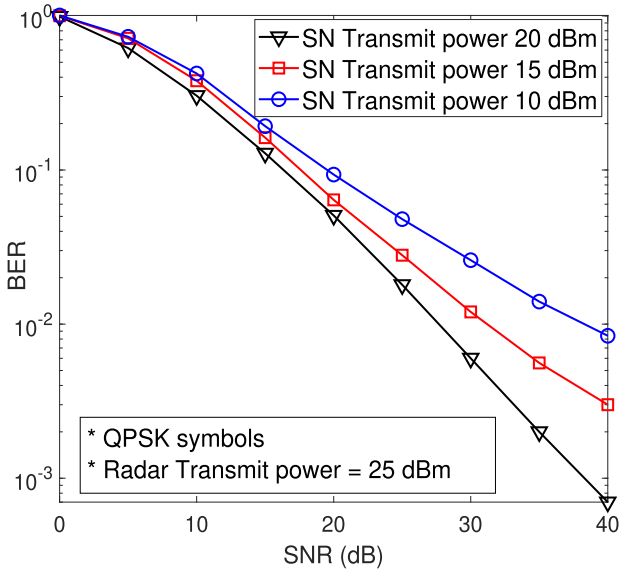

FIGURE 21. BER performance evaluation with respect to SNR at the DN, when radar power is fixed at 25 dBm.

SN power. This is expected as higher SN power counters the interference from radar at the RN and DN. We also observe the flattening of BER curve with higher of SINR as the RN and DN become interference dominated for a fixed radar power and the performance does not improve any further. This is more prominent at lower SN power of 10 dBm.

Note: MATLAB code is available in https://sites.google.com/view/portfolio-m-coding/home.

VII. CONCLUSION

In this study, we introduce a novel communication topology termed RadRCom, which integrates relay into a radar-communication systems with single antenna. Given the likelihood of link failures in automotive radar-communication applications due to channel unavailability, the inclusion of relays becomes crucial. We present two design problems for the RadRCom system. Firstly, we address radar waveform design by maximizing the SINR at the radar, and secondly, we delve into relay design by minimizing the MSE at the communication receiver. We find that the problem is non-convex in nature and complexity is high, and leads to sub-optimal solutions with mild degradation in performance. Theoretical analyses pertaining to radar detection and SER are conducted, with simulation results demonstrating satisfactory quality of service in terms of BER and MSE. We also observe BER/MSE performance recovery by using the proposed RadRCom compared to the conventional RadCom one, where link is poor. Moreover, we discuss the challenges in RadRCom system design. Future extensions of this work includes exploring MIMO systems, various relay model configurations, and addressing moving targets in radar systems.

REFERENCES

[1] A. Gupta and R. K. Jha, "A survey of 5G network: Architecture and emerging technologies," *IEEE Access*, vol. 3, pp. 1206–1232, 2015.
[2] R. Khan, P. Kumar, D. N. K. Jayakody, and M. Liyanage, "A survey on security and privacy of 5G technologies: Potential solutions, recent advancements, and future directions," *IEEE Commun. Surveys Tuts.*, vol. 22, no. 1, pp. 196–248, 1st Quart., 2020.
[3] M. Ashraf, B. Tan, D. Moltchanov, J. S. Thompson, and M. Valkama, "Joint optimization of radar and communications performance in 6G cellular systems," *IEEE Trans. Green Commun. Netw.*, vol. 7, no. 1, pp. 522–536, Mar. 2023.
[4] L. Zheng, M. Lops, Y. C. Eldar, and X. Wang, "Radar and communication coexistence: An overview: A review of recent methods," *IEEE Signal Process. Mag.*, vol. 36, no. 5, pp. 85–99, Sep. 2019.
[5] A. R. Chiriyath, B. Paul, and D. W. Bliss, "Radar-communications convergence: Coexistence, cooperation, and co-design," *IEEE Trans. Cognit. Commun. Netw.*, vol. 3, no. 1, pp. 1–12, Mar. 2017.
[6] A. K. Dutta, K. V. S. Hari, C. R. Murthy, N. B. Mehta, and L. Hanzo, "Minimum error probability MIMO-aided relaying: Multihop, parallel, and cognitive designs," *IEEE Trans. Veh. Technol.*, vol. 66, no. 6, pp. 5435–5440, Jun. 2017.
[7] Y. Ju, H. Wang, Y. Chen, T.-X. Zheng, Q. Pei, J. Yuan, and N. Al-Dhahir, "Deep reinforcement learning based joint beam allocation and relay selection in mmWave vehicular networks," *IEEE Trans. Commun.*, vol. 71, no. 4, pp. 1997–2012, Apr. 2023.
[8] Z. Wang, G. Liao, and Z. Yang, "Space-frequency modulation radar-communication and mismatched filtering," *IEEE Access*, vol. 6, pp. 24837–24845, 2018.
[9] P. Ren, A. Munari, and M. Petrova, "Performance tradeoffs of joint radar-communication networks," *IEEE Wireless Commun. Lett.*, vol. 8, no. 1, pp. 165–168, Feb. 2019.
[10] Y. Liu, G. Liao, J. Xu, Z. Yang, and Y. Zhang, "Adaptive OFDM integrated radar and communications waveform design based on information theory," *IEEE Commun. Lett.*, vol. 21, no. 10, pp. 2174–2177, Oct. 2017.
[11] F. Liu, C. Masouros, A. Li, and T. Ratnarajah, "Robust MIMO beamforming for cellular and radar coexistence," *IEEE Wireless Commun. Lett.*, vol. 6, no. 3, pp. 374–377, Jun. 2017.
[12] Z. Cheng, C. Han, B. Liao, Z. He, and J. Li, "Communication-aware waveform design for MIMO radar with good transmit beampattern," *IEEE Trans. Signal Process.*, vol. 66, no. 21, pp. 5549–5562, Nov. 2018.
[13] F. Liu, A. Garcia-Rodriguez, C. Masouros, and G. Geraci, "Interfering channel estimation in radar-cellular coexistence: How much information do we need?" *IEEE Trans. Wireless Commun.*, vol. 18, no. 9, pp. 4238–4253, Sep. 2019.
[14] A. Hassanien, M. G. Amin, Y. D. Zhang, and F. Ahmad, "Dual-function radar-communications: Information embedding using sidelobe control and waveform diversity," *IEEE Trans. Signal Process.*, vol. 64, no. 8, pp. 2168–2181, Apr. 2016.
[15] D.-P. Xia, Y. Zhang, P. Cai, and L. Huang, "An energy-efficient signal detection scheme for a radar-communication system based on the generalized approximate message-passing algorithm and low-precision quantization," *IEEE Access*, vol. 7, pp. 29065–29075, 2019.
[16] J. Qian, M. Lops, L. Zheng, X. Wang, and Z. He, "Joint system design for coexistence of MIMO radar and MIMO communication," *IEEE Trans. Signal Process.*, vol. 66, no. 13, pp. 3504–3519, Jul. 2018.
[17] J. Qian, Z. He, N. Huang, and B. Li, "Transmit designs for spectral coexistence of MIMO radar and MIMO communication systems," *IEEE Trans. Circuits Syst. II, Exp. Briefs*, vol. 65, no. 12, pp. 2072–2076, Dec. 2018.
[18] K. Singh, S. Biswas, T. Ratnarajah, and F. A. Khan, "Transceiver design and power allocation for full-duplex MIMO communication systems with spectrum sharing radar," *IEEE Trans. Cognit. Commun. Netw.*, vol. 4, no. 3, pp. 556–566, Sep. 2018.
[19] B. Li, A. P. Petropulu, and W. Trappe, "Optimum co-design for spectrum sharing between matrix completion based MIMO radars and a MIMO communication system," *IEEE Trans. Signal Process.*, vol. 64, no. 17, pp. 4562–4575, Sep. 2016.
[20] E. Grossi, M. Lops, and L. Venturino, "Joint design of surveillance radar and MIMO communication in cluttered environments," *IEEE Trans. Signal Process.*, vol. 68, pp. 1544–1557, 2020.
[21] X. He and L. Huang, "Joint MIMO communication and MIMO radar under different practical waveform constraints," *IEEE Trans. Veh. Technol.*, vol. 69, no. 12, pp. 16342–16347, Dec. 2020.
[22] X. Yu, K. Alhujaili, G. Cui, and V. Monga, "MIMO radar waveform design in the presence of multiple targets and practical constraints," *IEEE Trans. Signal Process.*, vol. 68, pp. 1974–1989, 2020.

[23] Q. Zhang, Y. Zhou, L. Zhang, Y. Gu, and J. Zhang, "Waveform design for a dual-function radar-communication system based on CE-OFDM-PM signal," *IEEE Trans. Veh. Technol.*, vol. 69, no. 12, pp. 16342–16347, Apr. 2020.
[24] S. H. Dokhanchi, B. S. Mysore, K. V. Mishra, and B. Ottersten, "A mmWave automotive joint radar-communications system," *IEEE Trans. Aerosp. Electron. Syst.*, vol. 55, no. 3, pp. 1241–1260, Jun. 2019.
[25] L. G. de Oliveira, D. Brunner, A. Diewald, C. Muth, L. Schmalen, T. Zwick, and B. Nuss, "Bistatic OFDM-based joint radar-communication: Synchronization, data communication and sensing," in *Proc. 20th Eur. Radar Conf. (EuRAD)*, Sep. 2023, pp. 359–362.
[26] F. Liu, C. Masouros, A. Li, H. Sun, and L. Hanzo, "MU-MIMO communications with MIMO radar: From co-existence to joint transmission," *IEEE Trans. Wireless Commun.*, vol. 17, no. 4, pp. 2755–2770, Apr. 2018.
[27] Y. Ding, S. Yan, X. Zhou, F. Shu, and S. Feng, "Radar-communication waveform design with detection probability constraints," *IEEE Wireless Commun. Lett.*, vol. 12, no. 1, pp. 168–172, Jan. 2023.
[28] L. Chen, F. Liu, W. Wang, and C. Masouros, "Joint radar-communication transmission: A generalized Pareto optimization framework," *IEEE Trans. Signal Process.*, vol. 69, pp. 2752–2765, 2021.
[29] J. Zou, H. Luo, M. Tao, and R. Wang, "Joint source and relay optimization for non-regenerative MIMO two-way relay systems with imperfect CSI," *IEEE Trans. Wireless Commun.*, vol. 11, no. 9, pp. 3305–3315, Sep. 2012.
[30] C. Song, K.-J. Lee, and I. Lee, "MMSE based transceiver designs in closed-loop non-regenerative MIMO relaying systems," *IEEE Trans. Wireless Commun.*, vol. 9, no. 7, pp. 2310–2319, Jul. 2010.
[31] C. Xing, S. Ma, and Y.-C. Wu, "Robust joint design of linear relay precoder and destination equalizer for dual-hop amplify-and-forward MIMO relay systems," *IEEE Trans. Signal Process.*, vol. 58, no. 4, pp. 2273–2283, Apr. 2010.
[32] X. Sun, W. Yang, and Y. Cai, "Secure and reliable transmission in mmWave NOMA relay networks with SWIPT," *IEEE Syst. J.*, vol. 16, no. 3, pp. 4861–4872, Sep. 2022.
[33] A. G. Flattie, "Performance evaluation of MIMO cooperative radar by considering high altitude aeronautical platforms," in *Proc. Int. Conf. Challenges IT, Eng. Technol. (ICCIET)*, vol. 1, Jul. 2014, pp. 88–94.
[34] L. Zheng, M. Lops, Y. C. Eldar, and X. Wang, "Radar and communication co-existence: An overview," 2019, *arXiv:1902.08676*.
[35] P. E. Gill and E. Wong, "Sequential quadratic programming methods," in *Mixed Integer Nonlinear Programming*, J. Lee and S. Leyffer, Eds. New York, NY, USA: Springer, 2012, pp. 147–224.
[36] S. M. Key, *Fundamentals of Statistical Signal Processing: Detection Theory*, vol. 2. London, U.K.: Pearson, 1998.
[37] A. Papathanassiou and A. Khoryaev, "Cellular V2X as the essential enabler of superior global connected transportation services," *IEEE 5G Tech. Focus*, vol. 1, no. 2, pp. 1–4, Nov. 2017.
[38] J. Dai, X. Hao, P. Li, Z. Li, and X. Yan, "Antijamming design and analysis of a novel pulse compression radar signal based on radar identity and chaotic encryption," *IEEE Access*, vol. 8, pp. 5873–5884, 2020.

SOUMITA NASKAR (Graduate Student Member, IEEE) received the B.Tech. degree in electronics and telecommunication engineering from MAKAUT, West Bengal, India, and the M.Tech. degree from the Defence Institute of Advanced Technology, Pune, India. She is currently pursuing the Ph.D. degree with the G.S. Sanyal School of Telecommunications, Indian Institute of Technology at Kharagpur, India. Her current research interests include wireless communication systems design, radar system design, and quantum signal processing.

AMIT KUMAR DUTTA (Member, IEEE) received the B.E. degree in electronics and telecommunication engineering from IIEST, Shibpur, India, and the Ph.D. degree from Indian Institute of Science, Bengaluru, India. He is currently an Assistant Professor with the G.S. Sanyal School of Telecommunications, Indian Institute of Technology at Kharagpur, India. He has worked at Texas Instrument (TI) Pvt. Ltd., Broadcom Ltd., and Cypress Semiconductor and NxP Ltd., for a total of almost 14 years prior to joining academics. He has an elaborate work experience in the field of signal processing, communication and VLSI design in corporate, which included wireless system design and validation and characterization. His current research interests include wireless communication systems design, massive MIMO, OFDM, mmWave, and THz communications system design, and quantum signal processing.